Endothelin-1 activates a Ca^{2+}-permeable cation channel with TRPC3 and TRPC7 properties in rabbit coronary artery myocytes

C. M. Peppiatt-Wildman, A. P. Albert, S. N. Saleh and W. A. Large

Ion Channels and Cell Signalling, Division of Basic Medical Sciences, St George's, University of London, Cranmer Terrace, London SW17 ORE, UK

In the present work we used patch pipette techniques to study the properties of a novel Ca^{2+}-permeable cation channel activated by the potent coronary vasoconstrictor endothelin-1 (ET-1) in freshly dispersed rabbit coronary artery myocytes. With cell-attached recording bath application of 10 nM ET-1 evoked cation channel currents (I_{cat}) with subconductance states of about 18, 34 and 51 and 68 pS, and a reversal potential of 0 mV. ET-1 evoked channel activity when extracellular Ca^{2+} was the charge carrier, illustrating significant Ca^{2+} permeability. ET-1-induced responses were inhibited by the ET_A receptor antagonist BQ123 and the phospholipase C (PLC) inhibitor U73122. The diacylglycerol analogue 1-oleoyl-2-acetyl-*sn*-glycerol (OAG) also stimulated I_{cat}, but the protein kinase C (PKC) inhibitor chelerythrine did not inhibit either the OAG- or ET-1-induced I_{cat}. Inositol 1,4,5-trisphosphate (IP_3) did not activate I_{cat}, but greatly potentiated the response to OAG and this effect was blocked by heparin. Bath application of anti-TRPC3 and anti-TRPC7 antibodies to inside-out patches markedly inhibited ET-1-evoked I_{cat}, but antibodies to TRPC1, C4, C5 and C6 had no effect. Immunocytochemical studies demonstrated preferential TRPC7 expression in the plasmalemma, whereas TRPC3 was distributed throughout the myocyte, and moreover co-localization of TRPC3 and TRPC7 signals was observed at, or close to, the plasma membrane. Flufenamic acid, Gd^{3+}, La^{3+} and extracellular Ca^{2+} inhibited I_{cat} with IC_{50} values of 2.45 μM, 3.8 μM, 7.36 μM and 22 μM, respectively. These results suggest that in rabbit coronary artery myocytes ET-1 evokes a Ca^{2+}-permeable non-selective cation channel with properties similar to TRPC3 and TRPC7, and indicates that these proteins may be important components of this conductance.

(Received 14 December 2006; accepted after revision 15 February 2007; first published online 15 February 2007)
Corresponding author A. P. Albert: Ion Channel and Cell Signalling, Division of Basic Medical Sciences, St George's, University of London, Cranmer Terrace, London SW17 ORE, UK. Email: aalbert@sgul.ac.uk

Endothelin-1 (ET-1) is a 21-amino acid peptide which produces potent and persistent vasoconstriction (Yanagisawa *et al.* 1988) and has been linked to inappropriate vasoconstriction in coronary artery disease (see Schiffrin & Touyz, 1998). ET-1 tonically constricts human coronary arteries, especially those with atherosclerosis, and is responsible for resting tone at coronary artery stenoses (Kinlay *et al.* 2001). Plasma levels of ET-1 are elevated in patients with coronary artery disease (Matsuyama *et al.* 1991; Toyo-oka *et al.* 1991), and there are significant amounts of ET-1 in the intima of human atherosclerotic coronary arteries (Lerman *et al.* 1991, 1995). Consequently there is substantial evidence for a pathophysiological role for ET-1 in coronary artery vasoconstriction, and therefore a greater understanding of the cellular mechanisms underlying the ET-1-evoked response may provide improved clinical treatments for coronary artery disease.

ET-1 acts directly on vascular smooth muscle cells primarily via ET_A receptors, although ET_B receptors may also produce contraction (Davenport & Battistini, 2002). ET-1 produces an increase in intracellular Ca^{2+} concentration $[Ca^{2+}]_i$, which is essential for the ET-1-induced vasoconstriction (see review by Miwa *et al.* 2005). Moreover the majority of the contractile response is mediated by the influx of Ca^{2+} ions, but this does not involve classical voltage-gated Ca^{2+} channels (VGCCs, Miwa *et al.* 2005). Consequently ET-1 may activate Ca^{2+}-permeable cation channels, and candidates for this mechanism are classical transient receptor potential channels (TRPCs), which are widely distributed in vascular smooth muscle, and may mediate vasoconstrictor

 DOI: 10.1113/jphysiol.2006.126656

responses to many endogenous mediators (Large, 2002; Beech *et al.* 2004; Albert & Large, 2006).

Recently, Ko *et al.* (2004), using whole-cell recording, demonstrated that ET-1 evoked a non-selective cation current in rabbit coronary artery myocytes. A drawback of this approach is that ET-1 may stimulate several cation conductances which contribute to the whole-cell current. It has been shown that noradrenaline evokes two distinct non-selective cation channels in rabbit portal vein (see Albert & Large, 2006) and angiotensin II also activates two conductances in rabbit mesenteric artery myocytes (Saleh *et al.* 2006). Consequently there are serious limitations to the conclusions from measuring solely whole-cell currents. To overcome this problem we have measured directly single-channel activity evoked by ET-1 in rabbit coronary artery myocytes. We describe the properties of ET-1-evoked cation channels and provide evidence that TRPC7, possibly as a heterotetramer with TRPC3, is an important component of the ET-1-induced conductance.

Methods

Cell isolation

New Zealand White rabbits (2–3 kg) were killed by an I.V. injection of sodium pentobarbitone (120 mg kg^{-1}; in accordance with the UK Animals Scientific Procedures Act, 1986) and the left main, left anterior descending and right coronary arteries were removed and cleaned and dispersed into single smooth muscle cells using enzymatic procedures and solutions previously described (Saleh *et al.* 2006).

Electrophysiology

Single cation channel currents were recorded with an AXOPATCH 200B patch-clamp amplifier (Axon Instruments, Inc., CA, USA) at room temperature (20–23°C) using cell-attached, inside-out and outside-out patch configurations of the patch-clamp technique (Hamill *et al.* 1981). Patch pipettes were manufactured from borosilicate glass and then fire polished to produce pipettes with resistances of about 6–10 MΩ for isolated patch recording when filled with patch pipette solution. To reduce 'line' noise, the recording chamber (volume ~ 150–200 μl) was perfused using two 20 ml syringes, one filled with external solution and the other used to drain the chamber, in a 'push and pull' technique. The external solution could be exchanged twice within 30 s. When recording single-channel currents, the holding potential was routinely set at −50 mV, and to the evaluate *I–V* characteristics of single-channel currents, the membrane potential was manually changed between −50 mV and +50 mV.

Single-channel currents were initially recorded onto digital audiotape (DAT) using a digital tape-recorder (DRA-200; BioLogic Science Instruments, France) at a bandwidth of 5 kHz (AXOPATCH 200B patch-clamp amplifier) and a sample rate of 48 kHz. For off-line analysis, single cation channel records were filtered at 1 kHz (see below, −3 dB, low-pass 8-pole Bessel filter, Frequency Devices, model LP02, Scensys Ltd, Aylesbury, UK) and acquired using a Digidata 1322A and pCLAMP 9.0 at a sampling rate of 10 kHz, respectively. Data were captured with a Dimension 5150 personal computer (Dell, UK).

Single-channel current amplitudes were calculated from idealized traces of at least 10 s duration, using the 50% threshold method with events lasting for < 0.664 ms ($2\times$ rise time for a 1 kHz (−3 dB) low-pass filter) being excluded from analysis (Colquhoun, 1987). Figure preparation was carried out using MicroCal Origin software 6.0 (MicroCal Software Inc., MA, USA), where inward channel currents are shown as downward deflections. The number of channels in a patch was unknown, and therefore open probability (NP_o) was calculated using the equation: NP_o = total open time of all channel levels in the patch/sample recording.

Immunocytochemistry

Freshly dispersed myocytes were fixed with 70% ethanol in PBS (Sigma, UK) for 10 min at room temperature, washed with PBS and then permeabilized with PBS containing 0.5% Triton X-100 for 20 min at room temperature. After cells were incubated with PBS containing 10% chicken serum/donkey serum (relative to the species in which the secondary antibody was raised) and 0.1% Triton X-100 for 1 h at room temperature, the cells were then incubated with anti-TRPC antibodies (1 : 200 dilution) in PBS containing 10% chicken serum/donkey serum overnight at 4°C. The cells were then washed and incubated with secondary antibodies conjugated to a fluorescent probe (Alexa Fluor 488-conjugated chicken anti-rabbit antibody, 1 : 200; Alexa Fluor 555-conjugated donkey anti-goat antibody, 1 : 200). In control experiments, the primary antibodies were pre-incubated for 12 h at 4°C with antigenic peptide (1 : 25). After removing the unbound secondary antibodies by washing the preparations with PBS, the myocytes were imaged using laser scanning confocal microscope. Myocyte nuclei were labelled with DAPI mounting medium (Vector Shield, USA).

Confocal microscopy

The cells were imaged using a Zeiss LSM 510 laser scanning confocal microscope (Carl Zeiss, Jena, Germany). Excitation was produced by 488/405/543 nm lasers and delivered to the specimen via a Zeiss Apochromat ×63 oil-immersion objective (NA 1.4). Emitted fluorescence was captured using LSM 510 software (release 3.2, Carl Zeiss, Jena, Germany). A two-dimensional image of the

cells, cutting horizontally through approximately the middle of the cell, was captured (1024 × 1024 pixels).

Raw confocal imaging data were processed and analysed using Zeiss LSM 510 software. To assess the cellular distribution of TRPC channel proteins, a circular area of 0.78 μm^2 (diameter about 1 μm and referred to as Region 1) was randomly selected in the subplasmalemmal area of the cell so that its perimeter touched the edge of the cell from the inside. Another circular area of 0.78 μm^2 (Region 2) was selected so that the perimeter of the circle touched the perimeter of Region 1, and the line going through centres of these circles was perpendicular to the edge of the cell, thought to be the plasma membrane. A percentage of fluorescing pixels (%FP) was calculated in both regions using the formula:

$$\%\mathrm{FP} = 100 \times \frac{n(p > threshold)}{n(p)}$$

where $n(p >$ threshold) is the number of pixels within the region whose intensity equalled or exceeded the threshold value (one standard deviation, to exclude low-intensity pixels caused by photomultiplier noise) and $n(p)$ the total number of pixels in the region. The %FP values were then compared with each other and with the %FP in the whole confocal plane of the cell. The average pixel fluorescence (APF) value was used to compare the overall fluorescence signal between the staining and its controls and was calculated using the formula:

$$\mathrm{APF} = \frac{\sum i(p)}{n(p)} (\text{i.u./pixel})$$

where $i(p)$ is the intensity of a pixel within the confocal plane of the cell, and $n(p)$ is the total number of pixels of the plane. Statistical evaluation and graphs were created using Origin, and final images were produced using Powerpoint (Microsoft XP).

Solutions and drugs

The patch-pipette solution used for both cell-attached and inside-out patch recording (extracellular solution) was K^+-free and contained (mM): NaCl 126, $CaCl_2$ 1.5, Hepes 10, glucose 11, TEA 10, 4-AP 5, iberiotoxin 0.0002, DIDS 0.1, niflumic acid 0.1 and nicardipine 0.005, pH adjusted to 7.2 with NaOH. Under these conditions, VDCCs, K^+ currents, swell-activated Cl^- currents and Ca^{2+}-activated conductances are abolished, and non-selective cation currents can be recorded in isolation. In Ca^{2+}-permeability studies, NaCl was replaced with 90 mM $CaCl_2$. The pipette solution used for outside-out patch recording was K^+-free and contained (mM): CsCl 18, caesium aspartate 108, MgCl 1.2, Hepes 10, glucose 11, BAPTA 10, $CaCl_2$ 4.8 (free internal Ca^{2+} concentration approximately 100 nM as calculated using EQCAL software), Na_2ATP 1, NaGTP 0.2, pH adjusted to 7.2 with Tris.

In cell-attached patch experiments, the membrane potential was set to approximately 0 mV by perfusing cells in a KCl external solution containing (mM): KCl 126, $CaCl_2$ 1.5, Hepes 10 and glucose 11, pH adjusted to 7.2 with 10 M NaOH. Nicardipine (5 μM) was also included to prevent smooth muscle cell contraction by blocking Ca^{2+} entry through VDCCs. The composition of the bathing solution used in inside-out experiments (intracellular solution) was the same as the patch-pipette solution used for outside-out patch recording, except that 1 mM BAPTA and 0.48 mM $CaCl_2$ were included (free internal Ca^{2+} concentration approximately 100 nM). The bathing solution used in outside-out patch recording was K^+-free and contained (mM): NaCl 126, $CaCl_2$ 1.5, Hepes 10, glucose 11, DIDS 0.1, niflumic acid 0.1 and nicardipine 0.005, pH adjusted to 7.2 with NaOH. In some experiments, external 1.5 mM $CaCl_2$ was replaced with 10 μM, 100 μM or 10 mM $CaCl_2$, and in the Ca^{2+}-free external solution $CaCl_2$ was removed and 1 mM BAPTA was added (<10 nM free Ca^{2+}).

BQ123 was obtained from Calbiochem (UK), and all other drugs were purchased from Sigma (UK). Agents were dissolved in distilled H_2O or DMSO and 0.1% solution of DMSO alone had no effect on single-channel activity. Anti-TRPC antibodies raised against putative intracellular epitopes were obtained from Alomone Laboratories (Israel, TRPC1, C3, C4, C5 and C6) and Santa Cruz Biotechnology (USA, TRPC1, C3, C6 and C7).

The values are the mean of n cells ± S.E.M. Statistical analysis was carried out using paired (comparing effects of agents on the same cell) or unpaired (comparing effects of agents between cells) Student's t tests with the level of significance set at $P < 0.05$.

Results

ET-1 activates Ca^{2+}-permeable cation channels in coronary artery myocytes

We initially investigated the effect of ET-1 on freshly dispersed coronary artery myocytes using the cell-attached configuration of the patch-clamp technique, which does not cause perturbation of the intracellular milieu.

Figure 1*A* shows that bath application of 10 nM ET-1 activated inward channel currents at −50 mV with a mean open probability (NP_o) of 1.796 ± 0.319 ($n = 18$), and exhibited four distinct peak amplitude levels with discrete transitions between each level (Fig. 1*Aa* and *b*). Figure 1*Ac* illustrates the mean current–voltage relationship of ET-1-evoked inward channel currents, showing that the four peak amplitudes had unitary conductance states of 18, 34, 51 and 68 pS, which all had reversal potentials (E_r) of about 0 mV.

Using a patch pipette solution containing 90 mM $CaCl_2$/zero NaCl, bath application of 10 nM ET-1 activated inward channel currents with a mean NP_o of 0.099 ± 0.019 ($n = 5$) at −50 mV, which had four unitary conductance states of about 13, 23, 34 and 46 pS and E_r of about 0 mV. These results demonstrate that the ET-1-activated channel is permeable to Ca^{2+} ions.

The observation that in all patches tested, with both 126 mM NaCl/1.5 mM $CaCl_2$ and 90 mM $CaCl_2$ patch pipette solutions, ET-1-activated cation channel currents consisted of four current levels, that discrete transitions occurred between these four levels and that all four states had a similar E_r suggest that these levels relate to openings of a single channel with four subconductance states. However since the second, third and fourth levels were close multiples of the lower level, it is possible that all patches tested contained at least four cation channels and the different levels represented openings of multiple channels.

These data indicate that ET-1 activates a Ca^{2+}-permeable cation channel (I_{cat}) in coronary artery myocytes, but it should also be noted that ET-1 also activated a much smaller-amplitude cation channel (less than −0.2 pA at −50 mV), which was not studied in the present work. The observation that ET-1 activates more than one type of cation conductance in coronary artery myocytes further reinforces our approach of recording cation channel activity at the single-channel level.

Signal transduction pathways of ET-1-evoked I_{cat}

In vascular myocytes it is established that ET-1 acts on G-protein-coupled receptors which stimulate phospholipase C (PLC) to cleave phosphatidylinositol-4, 5-bisphosphate (PIP_2) to inositol-1,4,5-trisphosphate (IP_3) and diacylglycerol (DAG), and therefore we investigated the role of this biochemical cascade in ET-1-induced I_{cat}.

Figure 1*B* shows that in the presence of the selective ET_A receptor antagonist 100 nM BQ123, 10 nM ET-1 evoked only small activation of I_{cat}, but I_{cat} activity was markedly increased following washout of BQ123. In the presence of 100 nM BQ123, 10 nM ET-1 activated I_{cat} activity with a mean NP_o value of 0.014 ± 0.004, which was significantly increased to 1.082 ± 0.035 ($n = 7$, $P < 0.05$) following washout of BQ123. Figure 1*C* shows that bath application of the PLC inhibitor 10 μM U73122 significantly inhibited ET-1-evoked I_{cat} by $59 \pm 11\%$ ($n = 8$, $P < 0.05$), whereas its inactive analogue U73343 had no effect on I_{cat} ($n = 5$). Figure 1*D* illustrates that bath application of the protein kinase C (PKC) inhibitor 3 μM chelerythrine had no effect of ET-1-activated I_{cat} ($n = 5$).

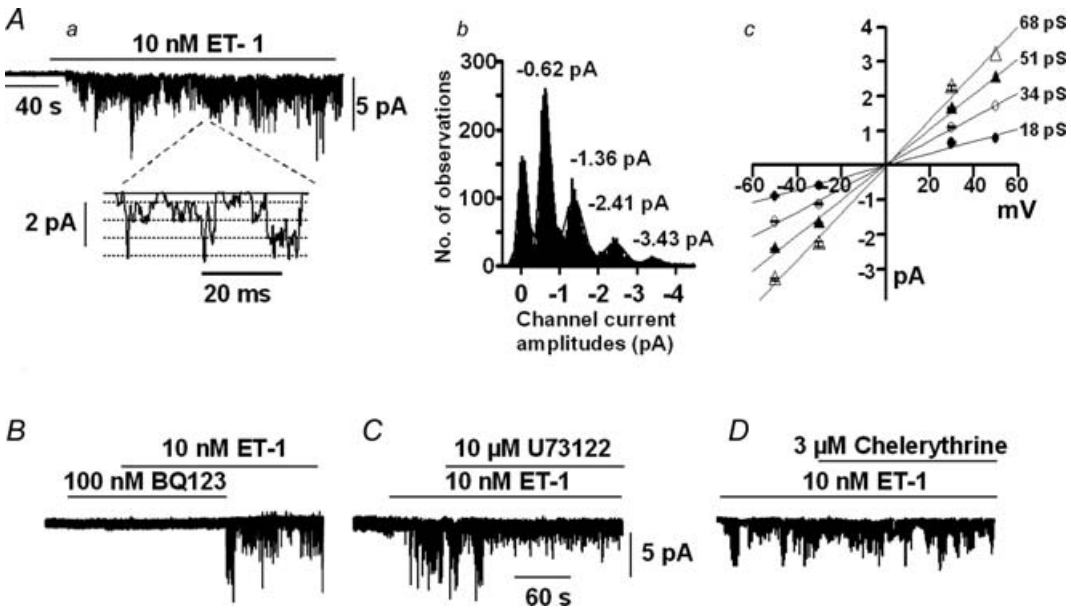

Figure 1. ET-1 activates a cation channel in cell-attached patches from coronary artery myocytes
Aa, bath application of 10 nM ET-1 evoked cation channel currents at −50 mV; *Ab*, the amplitude histogram of ET-1-evoked cation channel currents shown in *Aa* could be fitted by five Gaussian curves with peaks representing one closed and four open levels. *Ac*, mean current–voltage relationship of ET-1-induced cation channel currents showing the four peak amplitude levels had unitary conductances of 18, 34, 51 and 68 pS, which had E_r values of about 0 mV. Each point is from at least $n = 6$. *B*, pre-incubation with 100 nM BQ123 reduced ET-1-evoked I_{cat}, which was reversed following washout of BQ123. *C*, bath application of 10 μM U73122 reduced ET-1-evoked I_{cat}. *D*, bath application of 3 μM chelerythrine had no effect on ET-1-induced I_{cat}.

These data indicate that ET-1 induces I_{cat} activity in coronary artery myocytes through ET_A receptors coupled to U73122-sensitive PLC, but does not involve activation of PKC.

Role of DAG and IP_3 in evoking I_{cat}

We have shown that the two products of PIP_2 hydrolysis, DAG and IP_3, have important roles in activating native cation channels in portal vein, mesenteric artery and ear artery myocytes (see Albert & Large, 2006; Saleh *et al.* 2006), and therefore we studied the effect of these two agents on I_{cat} in inside-out patches from coronary artery myocytes.

Figure 2*Aa* and *b*, and *C* shows that bath application of the DAG analogue 1-oleoyl-2-acetyl-*sn*-glycerol (OAG, 10 μM) activated cation channel currents which displayed four peak amplitude levels with unitary conductances/E_r values similar to ET-1-evoked I_{cat} in cell-attached patches. Stimulation of I_{cat} by OAG was not inhibited by chelerythrine (3 μM, $n = 6$). Importantly, bath application of 10 μM IP_3 alone had no effect on I_{cat} activity but Fig. 2*Aa* and *C* show that co-application of 10 μM IP_3 in the presence of 10 μM OAG produced a marked increase in I_{cat} activity. The similarity between the peaks of the amplitude histograms produced in the presence of OAG (Fig. 2*Ab*) and OAG + IP_3 (Fig. 2*Ac*) provides evidence that IP_3 increased the activity of I_{cat} and did not activate a different channel. Figure 2*B* and *C* illustrates that the potentiating effect of IP_3 on DAG-evoked I_{cat} was inhibited by the IP_3 receptor antagonist heparin (1 mg ml^{-1}), but that a pronounced increase in I_{cat} activity by IP_3 was observed following washout of heparin.

These data suggest that DAG has an important role in activating I_{cat}, and that IP_3 increases I_{cat} activity via a heparin-sensitive binding site.

Molecular properties of I_{cat}

The properties of ET-1-induced I_{cat} in coronary artery myocytes are similar to those of cation channel currents described in the portal vein, mesenteric artery and ear artery in which TRPC channel proteins appear to be involved (see Albert & Large, 2006; Albert *et al.* 2006;

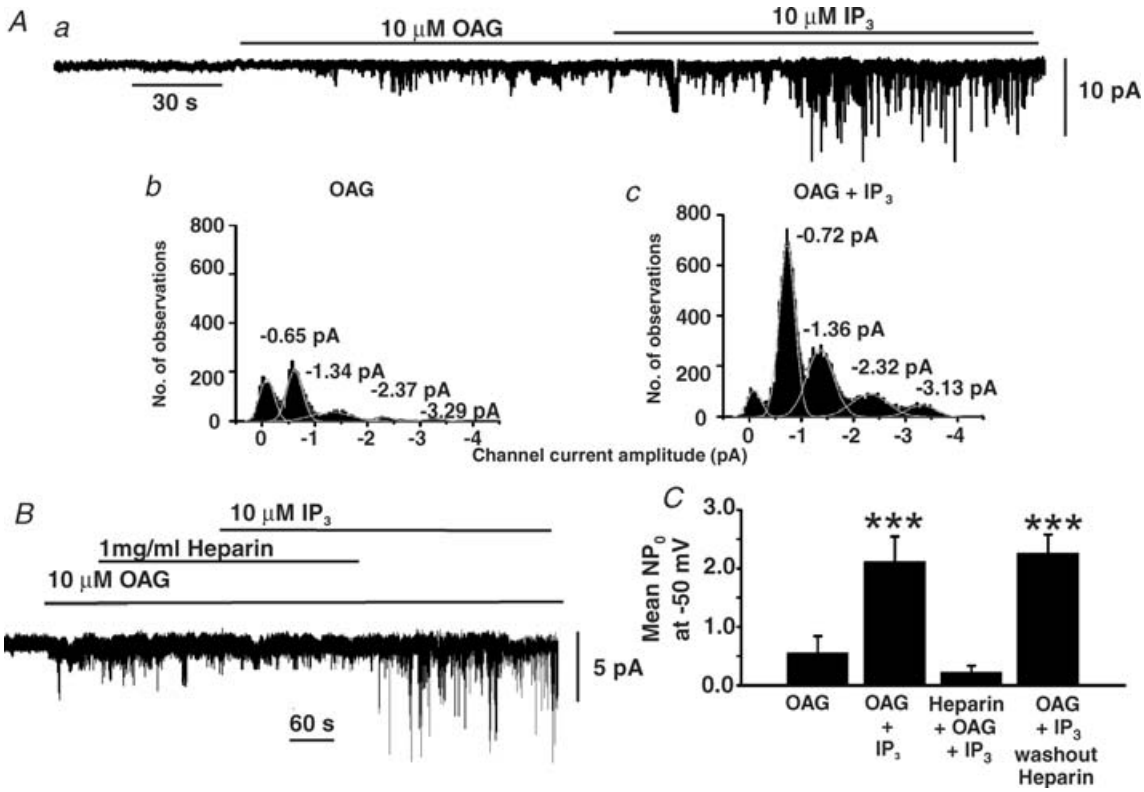

Figure 2. Effect of OAG and IP_3 on I_{cat} in inside-out patches
Aa, bath application of 10 μM OAG-activated I_{cat} and channel activity was markedly increased by co-application of 10 μM IP_3. *Ab* and *c*, the amplitude histograms evoked by OAG and OAG/IP_3 had similar peak amplitudes indicating that IP_3 potentiates the activity of the same channel. *B*, pre-incubation with 1 mg ml^{-1} heparin inhibited the potentiating effect of IP_3 on OAG-evoked I_{cat}, which was reversed following washout of heparin. *C*, mean data from these experiments ($n =$ at least 6, $^{***}P < 0.001$).

Saleh *et al.* 2006). Therefore we explored the role of TRPC channel proteins in mediating I_{cat}, by studying the effect of anti-TRPC antibodies and pharmacological agents on ET-1-evoked I_{cat}. In the former experiments, I_{cat} was activated in the cell-attached configuration by bath application of 10 nM ET-1, and then patches were excised into the inside-out configuration and anti-TRPC antibodies raised against intracellular epitopes were applied to the cytoplasmic surface of patches. In inside-out patches, I_{cat} activity was maintained during the lifetime of the recording (up to 20 min) with no evidence of run down. However, to provide further evidence for the robust nature of I_{cat} activity in inside-out patches, we regularly obtained some degree of reversibility following washout of anti-TRPC antibodies which inhibited I_{cat}.

Figure 3*Aa* and *b*, and *B* shows that bath application of both anti-TRPC7 and anti-TRPC3 antibodies produced pronounced inhibition of ET-1-evoked I_{cat} by over 80%. In addition Fig. 3*B* shows that when anti-TRPC7 and anti-TRPC3 antibodies were pre-incubated with their antigenic peptides, these agents had no effect on channel activity. Moreover Fig. 3*B* shows that bath application of anti-TRPC1, C4, C5 and C6 antibodies had no effect of ET-1-evoked I_{cat} activity.

Figure 3*Ca–d* shows the effect of agents known to affect expressed TRPC cation channel activity (see Table 1 in Albert *et al.* 2006) on ET-1-evoked I_{cat} activity in outside-out patches, which had similar properties to those described in cell-attached patches. Figure 3*a–d* shows that flufenemic acid (FFA), La^{3+} and Gd^{3+} inhibited ET-1-evoked I_{cat} activity, with IC_{50} values of 2.45 μM, 7.36 μM and 0.38 μM, respectively, and that reducing extracellular Ca^{2+} concentration markedly potentiated ET-1-induced I_{cat} activity, with an IC_{50} value of 22 μM.

Expression of TRPC3 and TRPC7 in coronary artery myocytes

The above properties of ET-1-evoked I_{cat} suggest that TRPC3 and TRPC7 channel proteins are important components of this channel, and therefore we investigated the expression of TRPC3 and TRPC7 proteins in coronary artery myocytes using immunocytochemistry and laser scanning confocal microscopy.

Figure 4*A*, *B* and *Da* shows intense staining of TRPC7 proteins predominantly distributed at the plasma membrane of coronary artery myocytes, whereas punctate staining for TRPC3 proteins occurred throughout the cell. Figure 4*Db* and *c* shows that staining for TRPC7 and TRPC3 proteins was inhibited by pre-incubation with their antigenic peptides, and that secondary antibodies alone had no significant staining. Figure 4*Ca* and *b* shows

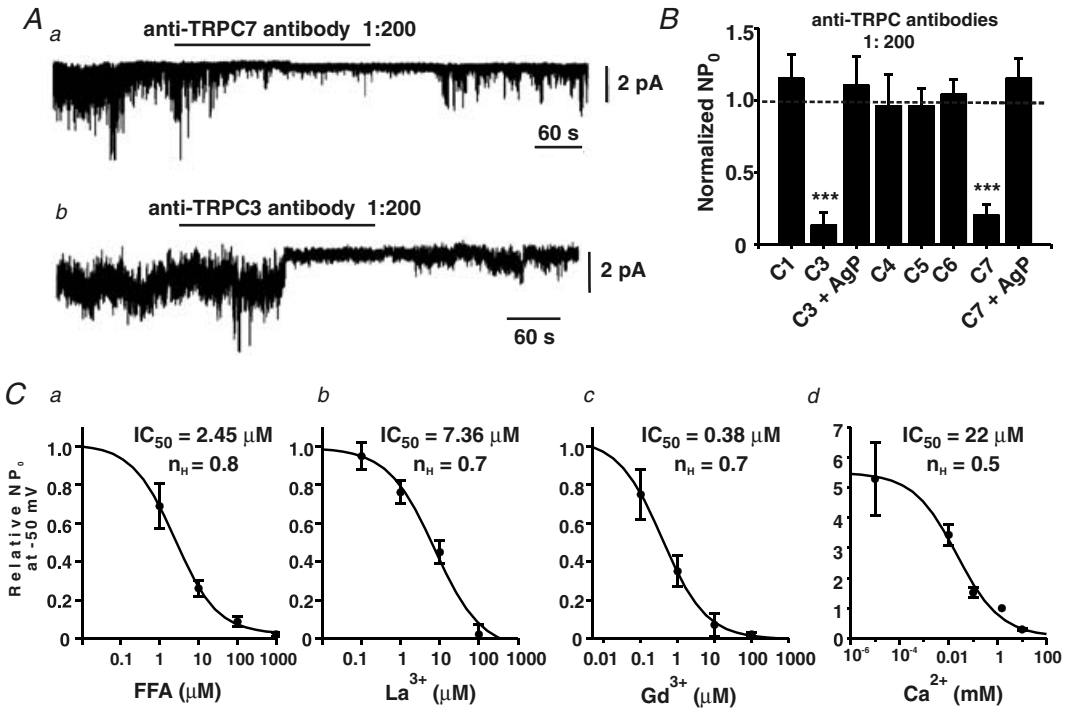

Figure 3. Effect of anti-TRPC antibodies and pharmacological agents on ET-1-evoked I_{cat}
Aa and *b*, bath application of anti-TRPC7 and anti-TRPC3 antibodies (1 : 200 dilution) inhibited ET-1-induced I_{cat} in inside-out patches. *B*, effect of anti-TRPC antibodies on the relative mean NP_o of ET-1-evoked I_{cat} (n = at least 6, $P < 0.01$). *C*, effect of FFA (*a*), La^{3+} (*b*), Gd^{3+} (*c*) and extracellular Ca^{2+} concentration (*d*) on ET-1-evoked I_{cat} in outside-out patches.

superimposed images of the myocyte in Fig. 4*A* and *B*. The staining patterns of anti-TRPC3 and TRPC7 antibodies indicate possible co-localization of TRPC3 and TRPC7 proteins specifically at the plasma membrane (shown in yellow).

Discussion

In the present work we describe the properties of a novel ET-1-activated Ca^{2+}-permeable cation channel in freshly dispersed rabbit coronary artery myocytes, and demonstrate that TRPC7, possibly in combination with TRPC3, forms an important constituent of the ion channel. To our knowledge this is the first evidence for a role for TRPC7 in native vascular myocytes.

Biophysical properties of ET-1-induced I_{cat}

ET-1-activated I_{cat} exhibited four conductance states of about 18, 34, 51 and 68 pS, which all had E_r values of approximately 0 mV in cell-attached, inside-out and outside-out patches. Moreover, in the presence of external 90 mM $CaCl_2$, when Ca^{2+} ions will be the main cation charge carrier, ET-1-induced I_{cat} also had four conductance states, albeit with lower values, of about 13, 23, 34 and 46 pS, which also all had E_r values of 0 mV. These data strongly indicate that ET-1-activated I_{cat} in coronary artery myocytes has significant permeability to Ca^{2+} ions. Since ET-1 always activated cation channel currents with four conductance states; discrete transitions were observed to occur between all these four levels; and all four conductance states had a similar E_r, this suggests that these multiple conductance levels relate to openings of a single channel with four subconductance states. However, since the second, third and fourth levels were close, but not purely additive, it is possible that that these different conductance states represent openings of multiple channels. However, it should be noted that for the four conductances states to be produced by openings of multiple channels, at least four channels (on occasions more) must have been present in each patch recorded from during the study.

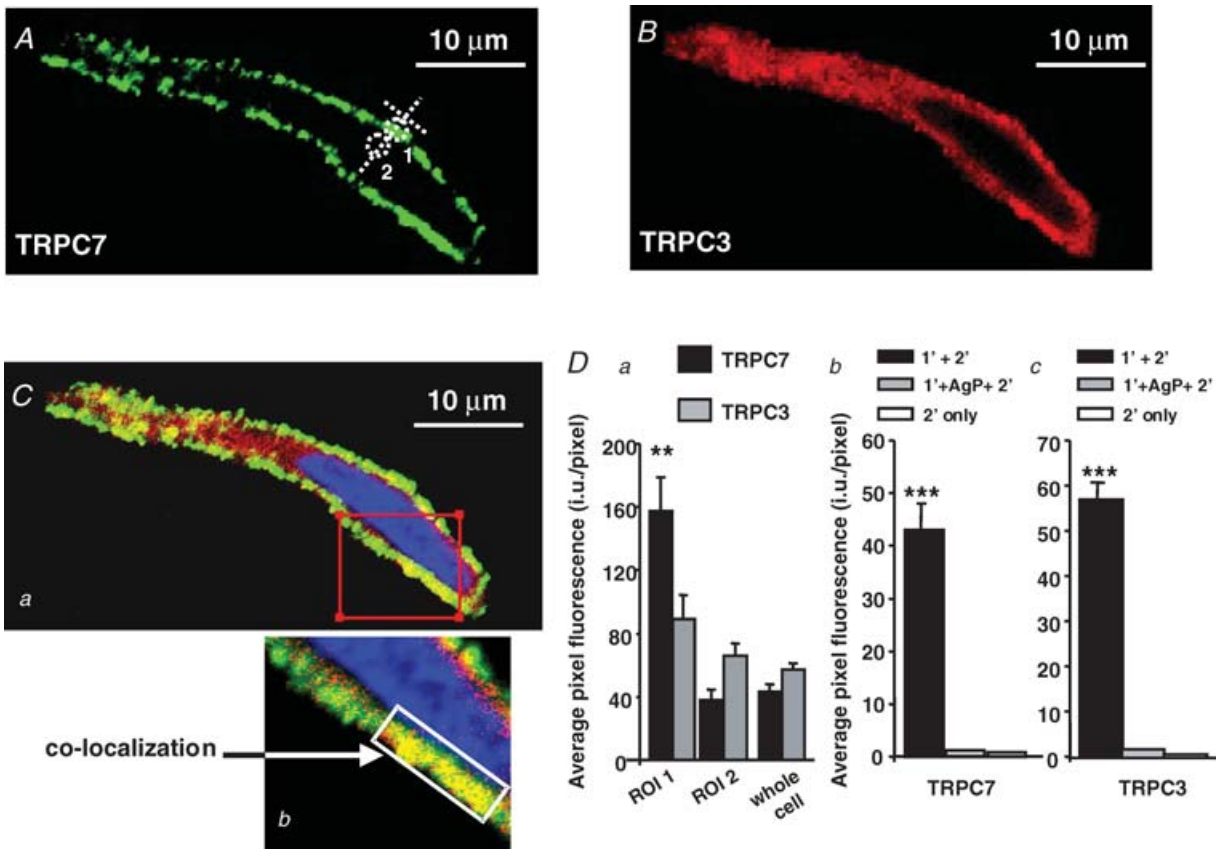

Figure 4. Expression of TRPC3 and TRPC7 channel proteins in coronary artery myocytes
A and *B*, staining of TRPC7 (green) and TRPC3 (red) proteins from a coronary artery myocyte. *C*, superimposition of staining for TRPC7 and TRPC3 proteins from the cell shown in *A*. Note in the inset the observation of co-localization between TRPC7 and TRPC3 staining (yellow) at the plasma membrane. *D*, mean data from these experiments (n = at least 10; $^{**}P < 0.01$; $^{***}P < 0.001$); ROI, region of interest; 1′ primary ab; 2′, secondary ab.

Signal transduction mechanism of ET-1-induced I_{cat}

The signal transduction mechanism linking ET-1 to activation of I_{cat} involves ET_A receptors coupled, at least partially, to U73122-senstive PLC. However, 10 μM U73122 only produced partial inhibition of ET-1-evoked I_{cat}, whereas 2 μM U73122 produced greater than 90% inhibition of noradrenaline-induced I_{cat} in the rabbit portal vein (Helliwell & Large, 1997) and angiotensin II-stimulated I_{cat} in rabbit mesenteric myocytes (Saleh *et al.* 2006). Consequently another isoform of PLC which is insensitive to U73122 also may link ET-1 receptors to channel opening, or another phospholipase may couple the ET-1 receptor to the ion channel, which is the case in rabbit ear artery myocytes where a constitutively active I_{cat} with TRPC3 properties is activated by DAG generated by phospholipase D (Albert *et al.* 2005, 2006).

It is demonstrated that the DAG analogue OAG activated I_{cat}, which was not blocked by the PKC inhibitor chelerythrine, and which also did not reduce ET-1-evoked I_{cat}. Thus it appears that DAG evokes I_{cat} via a PKC-independent mechanism. It is interesting that the ET-1-evoked whole-cell current in the same preparation was reduced by 50–60% by PKC inhibitors (Ko *et al.* 2004). Since the ET-1-evoked channel currents described in the present work were unaffected by PKC inhibitors, this indicates that the whole-cell current recorded by Ko *et al.* (2004) may have comprised several cation conductances as previously suggested (see Introduction). IP_3 alone did not evoke I_{cat}, but produced marked potentiation of OAG-evoked I_{cat}, and this effect was blocked by the IP_3 receptor antagonist heparin. Thus it is possible that both products of phosphoinositide (PI)- PLC activity, DAG and IP_3, are involved in activation of ET-1-evoked I_{cat}, which has also been shown for the noradrenaline-evoked TRPC6-like and store-operated channels in rabbit portal vein myocytes (Albert & Large, 2003; Liu *et al.* 2005) but not the TRPC6 channel currents in rabbit mesenteric artery (Saleh *et al.* 2006).

Molecular properties of ET-1-evoked I_{cat}

There is strong evidence that TRPC7 proteins are an important component of I_{cat}. Anti-TRPC7 anitibodies produced marked inhibition of I_{cat}, and this effect was blocked by pre-incubation with its antigenic peptide. Anti-TRPC7 antibodies did not affect TRPC3 channels in rabbit ear artery myocytes (Albert *et al.* 2006) or TRPC1 and TRPC6 channels in rabbit mesenteric artery myocytes (Saleh *et al.* 2006). Therefore the action of the anti-TRPC7 antibody is not due to a non-specific effect on cation channels. In agreement with TRPC7 properties, I_{cat} was activated by OAG by a PKC-independent mechanism similar to expressed TRPC7 (Okada *et al.* 1999). Moreover, also similar to expressed TRPC7 channels, I_{cat} exhibited a conductance level of about 70 pS, was potentiated by IP_3 (Vasquez *et al.* 2006) and was reduced by increasing extracellular Ca^{2+} concentration and FFA (Okada *et al.* 1999; Inoue *et al.* 2001). Finally, immunocytochemical studies showed that TRPC7 immunoreactivity was preferentially localized in the plasmalemma as expected of a receptor-operated ion channel. These data are strong evidence that TRPC7 proteins contribute to the ET-1-evoked I_{cat}.

Anti-TRPC3 antibody also reduced ET-1-induced channel activity, and this effect was blocked by pretreatment with its antigenic peptide. Anti-TRPC3 antibodies blocked constitutive channel activity in rabbit ear artery myocytes (Albert *et al.* 2006), but had no effect on cation conductances with TRPC1 and TRPC6 properties in rabbit mesenteric artery (Saleh *et al.* 2006). However, the immunocytochemical experiments illustrated distribution of TRPC3 throughout the cell, unlike its preferential distribution in the plasmalemma in rabbit ear artery where it functions as a constitutive channel that can also be stimulated by noradrenaline (Albert *et al.* 2003, 2006). Nevertheless the data with anti-TRPC3 antibodies on I_{cat} in coronary artery myocytes raises the question of whether the functioning channel consists of a heterotetramer of TRPC3 and TRPC7 subunits. It has been shown that this co-assembly of TRPC3 and TRPC7 subunits readily occurs (Goel *et al.* 2002; Hofmann *et al.* 2002). It was not possible to carry out co-immunoprecipitation studies to test this hypothesis because of the very small amount of coronary artery tissue. However confocal imaging indicated that there was some degree of co-localization of TRPC3 and TRPC7. Also there was no evidence for two different channels, and both anti-TRPC3 and anti-TRPC7 antibodies produced greater than 90% inhibition of I_{cat} in some patches, indicating that both antibodies recognized important constituents of the functioning channel. Hence it is possible that both TRPC3 and TRPC7 subunits contribute to the ET-1-induced I_{cat} in rabbit coronary artery myocytes. Previously it has been suggested that heteromultimeric TRPC6–TRPC7 channels contribute to a receptor-operated channel in cultured A7r5 cells (Maruyama *et al.* 2006), but the present report is the first concerning a role for TRPC7 in native arterial myocytes.

It should be noted that these anti-TRPC antibodies have not been tested against TRPC channel activity in expression systems, although our data indicate that these antibodies display a high degree of selectivity against native cation channel currents in vascular smooth muscle (see Albert *et al.* 2003; Saleh *et al.* 2006 and present data). Moreover, results regarding activation (e.g. DAG activation), regulation (e.g. IP3 and PKC) and pharmacology provide further evidence that these anti-TRPC antibodies are producing effects via interaction with their selective target proteins.

Pharmacology of ET-1-activated I_{cat}

Pharmacological analysis showed that FFA, Gd^{3+} and La^{3+} blocked the ET-1-induced channel currents, which is similar to TRPC3 and TRPC7 channels. The inhibitory effect of FFA is characteristic of TRPC3 and TRPC7, and provides further evidence against a role for TRPC6 which is potentiated by this agent (Inoue *et al.* 2001). Also it is interesting that the IC_{50} values of Gd^{3+} and La^{3+} against ET-1-induced channels in the coronary artery are intermediate between native/expressed TRPC3 and TRPC7 (see Table 1 in Albert *et al.* 2006) and that the inhibitory effect of extracellular Ca^{2+} ions on I_{cat} was more potent than on constitutively active TRPC3 channels in the ear artery (Albert *et al.* 2006). These data show that the conductance activated by ET-1 in coronary artery myocytes shows both TRPC3 and TRPC7 properties.

Diversity of TRPC channels in vascular smooth muscle

It is becoming increasingly apparent that there is marked diversity of TRPC channels, which are stimulated by vasoconstrictor agents in vascular smooth muscle. TRPC6 is activated by noradrenaline in rabbit portal vein myocytes (Inoue *et al.* 2001) and by angiotensin II in rabbit mesenteric artery (Saleh *et al.* 2006). However, there are distinct differences in the properties of these two TRPC6 channels, indicating two different TRPC6 isoforms in these preparations (see Discussion of Saleh *et al.* 2006 for details). Also, in rabbit mesenteric artery myocytes, angiotensin II stimulates a channel which comprises TRPC1 subunits (Saleh *et al.* 2006). In rabbit ear artery myocytes, noradrenaline increases the activity of constitutively active TRPC3 channels (Albert *et al.* 2003, 2006). Pyrimidine also activates TRPC3 channels in cerebral arteries (Reading *et al.* 2005). The present work shows that ET-1 evokes a conductance with TRPC3/TRPC7 characteristics in the rabbit coronary artery. Since these channels have significantly different pharmacology (see Table 1 in Albert *et al.* 2006 and present data), a reasonable expectation is that novel pharmacological agents may be developed in the treatment of important vascular diseases.

Conclusions

These results describe the properties of a novel ET-1-activated Ca^{2+}-permeable cation channel which is likely to contribute to coronary artery vasoconstriction, and it appears that TRPC7, possibly as a heterotetramer with TRPC3, is an important component of this ion channel. The properties of this TRPC channel are significantly different from the characteristics of previously described TRPC channels in vascular smooth muscle.

References

Albert AP & Large WA (2003). Synergism between inositol phosphates and diacylglycerol on native TRPC6-like channels in rabbit portal vein myocytes. *J Physiol* **552**, 789–795.

Albert AP & Large WA (2006). Transduction pathways and gating mechanisms of native TRP-like channels in vascular myocytes. *J Physiol* **570**, 45–51.

Albert AP, Piper AS & Large WA (2003). Properties of a constitutively active Ca^{2+}-permeable non-selective cation channel in rabbit ear artery myocytes. *J Physiol* **549**, 143–156.

Albert AP, Piper AS & Large WA (2005). Role of phospholipase D and diacylglycerol in activating constitutive TRPC-like cation channels in rabbit ear artery myocytes. *J Physiol* **566**, 769–780.

Albert AP, Pucovsky V, Prestwich SA & Large WA (2006). TRPC3 properties of a native constitutively active Ca^{2+}-permeable cation channel in rabbit ear artery myocytes. *J Physiol* **571**, 361–369.

Beech DJ, Muraki K & Flemming R (2004). Non-selective cationic channels of smooth muscle and the mammalian homologues of *Drosophilia* TRP. *J Physiol* **559**, 685–706.

Colquhoun D (1987). Practical analysis of single channel records. In *Microelectrode Techniques*, ed. Standen NB, Gray PTA & Whitaker MS, pp. 83–104. The Company of Biologists, Cambridge, UK.

Davenport AP & Battistini B (2002). Classification of endothelin receptors and antagonists in clinical development. *Clin Sci* **103**, 15–35.

Goel M, Sinkins WG & Schilling WP (2002). Selective association of TRPC channel subunits in rat brain synaptosomes. *J Biol Chem* **277**, 48303–48310.

Hamill OP, Marty A, Neher E, Salcmann B & Sigworth FJ (1981). Improved patch-clamp techniques for high-resolution current recording from cells and cell-free membrane patches. *Pflugers Arch* **391**, 85–100.

Helliwell RM & Large WA (1997). α1-Adrenoceptor activation of a non-selective cation current in rabbit portal vein by 1,2-diacyl-*sn*-glycerol. *J Physiol* **499**, 417–428.

Hofmann T, Schaefer M, Schultz G & Gudermann T (2002). Subunit composition of mammalian transient receptor potential channels in living cells. *Proc Natl Acad Sci U S A* **99**, 7461–7466.

Inoue R, Okada T, Onoue H, Harea Y, Shimizu S, Naitoh S, Ito Y & Mori Y (2001). The transient receptor potential protein homologue TRP6 is the essential component of vascular α-adrenoceptor-activated Ca^{2+}-permeable cation channel. *Circ Res* **88**, 325–337.

Kinlay S, Behrendt D, Wainstein M, Beltrame Fang JC, Creager MA, Selwyn AP & Ganz P (2001). Role of endothelin-1 in the active constriction of human atherosclerotic coronary arteries. *Circulation* **104**, 1114–1118.

Ko EA, Park WS & Earm YE (2004). Extracellular Mg^{2+} blocks endothelin-induced contraction through the inhibition of non-selective cation channels in coronary smooth muscle. *Pflugers Arch* **449**, 195–204.

Large WA (2002). Receptor-operated Ca^{2+}-permeable non-selective cation channels in vascular smooth muscle: a physiologic perspective. *J Cardiovasc Electrophysiol* **13**, 493–501.

Lerman A, Edwards BS, Hallett JW, Heublein DM, Sandberg SM & Burnett JC (1991). Circulating and tissue endothelin immunoreactivity in advanced atherosclerosis. *N Engl J Med* **325**, 997–1001.

Lerman A, Holmes DR, Bell MR, Garrett KN, Nishimura RA & Burnett JC (1995). Endothelin in coronary endothelial dysfunction and early atherosclerosis in humans. *Circulation* **92**, 2426–2431.

Liu M, Albert AP & Large WA (2005). Facilitatory effect of Ins(1,4,5)P_3 on store-operated Ca^{2+}-permeable cation channels in rabbit portal vein myocytes. *J Physiol* **566**, 161–171.

Maruyama Y, Nakanishi Y, Walsh EJ, Wilson DP, Welsh DG & Cole WC (2006). Heteromultimeric TRPC6–TRPC7 channels contribute to arginine vasopressin-induced cation current of A7r5 vascular smooth muscle cells. *Circ Res* **98**, 1520–1527.

Matsuyama K, Yasue M, Okumura K, Saito Y, Nakao K, Shirakami G & Imura H (1991). Increased plasma level of endothelin-1-like immunoreactivity during coronary spasm in patients with coronary spastic angina. *Am J Cardiol* **68**, 991–995.

Miwa S, Kawanabe Y, Okamoto Y & Masaki T (2005). Ca^{2+} entry involved in endothelin-1-induced contractions of vascular smooth muscle cells. *J Smooth Muscle Res* **41**, 61–75.

Okada T, Inoue R, Yamazaki K, Maeda A, Kurosaki T, Yamakuni T, Tanaka I, Shimizu S, Ikenaka K, Imoto K & Mori Y (1999). Molecular and functional characterization of a novel mouse transient receptor potential protein homologue TRP7. Ca^{2+}-permeable cation channel that is constitutively activated and enhanced by stimulation of G-protein coupled receptor. *J Biol Chem* **274**, 27359–27370.

Reading SA, Earley S, Walden BJ, Welsh DG & Brayden JE (2005). TRPC3 Mediates pyrinidine receptor-induced depolarisation of cerebral arteries. *Am J Physiol* **288**, H2055–H2061.

Saleh SN, Albert AP, Peppiatt CM & Large WA (2006). Angiotensin II activates two cation conductances with distinct TRPC1 and TRPC6 channel properties in rabbit mesenteric artery myocytes. *J Physiol* **577**, 479–495.

Schiffrin EL & Touyz RM (1998). Vascular biology of endothelin. *J Cardiovasc Pharmacol* **32**, S2–S13.

Toyo-oka T, Aizawa T, Suzuki N, Hirata Y, Miyauchi T, Shin WS, Yanagisawa M, Masaki T & Sugimoto T (1991). Increased plasma level of endothelin-1 and coronary spasm induction in patients with vasospastic angina pectoris. *Circulation* **83**, 476–483.

Vasquez G, Bird Gst. J, Mori Y & Putney JW Jr (2006). Native TRPC7 channel activation by an inositol trisphosphate receptor-dependent mechanism. *J Biol Chem* **281**, 25250–25258.

Yanagisawa M, Kurihara H, Kimura S, Tomobe Y, Kobayashi M, Mitsui Y, Yazaki Y, Goto K & Masaki T (1988). A novel potent vasoconstrictor peptide produced by vascular endothelial cells. *Nature* **332**, 441–415.

Acknowledgements

This work was supported by The Wellcome Trust and the British Heart Foundation. We thank Professor T. B. Bolton for use of his confocal microscope and facilities funded by The Wellcome Trust (grant no. 074724/Z/04/Z).